Aedes aegypti Aag-2 culture cells enter endoreplication process upon pathogen challenge

Christian Domínguez-Benítez[1], Javier Serrato-Salas[1], Renaud Condé, Humberto Lanz-Mendoza[1]

[1]Laboratorio de Infección e Inmunidad. Centro de Investigaciones sobre Enfermedades Infecciosas. Instituto Nacional de Salud Pública, Av. Universidad 655, CP 62100. Cuernavaca, Morelos, México.

Corresponding authors: humberto@insp.mx

Abstract

Metamorphic insects apparently rely on a finite number of cells after emergence to counterbalance either commensal and pathogen presence. For hematophagous insects, blood-feeding is a crucial step for offspring development, therefore enteric cells repairing molecular mechanisms consists in fine regulated pathways to counterattack biotic and abiotic insults. Nevertheless, recent research suggests that midgut cells are capable to adapt their immune responses to pathogen challenges. Recently, *Anopheles* and *Aedes* mosquitoes have been observed to increase their DNA cell content upon encounter with parasites, bacteria and virus respectively. Genomic endoreplication is one of the most important processes in larval development for fast transcriptional activity and protein secretion.

So, in this paper we explore the ability of *Aedes aegypti* Aag-2 culture cells to develop a likely endoreplication process to face pathogen presence.

Aag-2 cells at 6 and 12 hours post-biotic insult enter a proliferation arrest and increases DNA content, these two phenomena recovers control levels at 24 h post-treatment. It requires more research data about the type of genomic regions that has been replicated in the process, and the concentration that antimicrobial molecules are released into culture media.

Introduction

Host biological responses against invading pathogens relies on inducible and constitutive responses, humoral and cellular components, divided into innate and adaptive responses (Sprent, 1994). Typical innate peripheral cells are NK and monocyte/macrophages and dendritic cells (Weavers, Evans, Martin, & Wood, 2016); humoral defenses comprise antibody production and complement system, besides a large families of molecules with antimicrobial properties (Burnet, 1976). In invertebrates, host responses against invading pathogens relies on limited resources through innate responses like phagocytosis, nodule formation, encapsulation, reactive oxygen species local responses and antimicrobial peptides production (Barnard, Nijhof, Fick, Stutzer, & Maritz-Olivier, 2012; Costa, Jan, Sarnow, & Schneider, 2009; De Gregorio, Spellman, Tzou, Rubin, & Lemaitre, 2002; Dong et al., 2006; Hillyer, 2010; Kleino, 2010). These immune responses are controlled mainly by four transcriptional cascades, Toll, IMD, Jak/STAT and RNAi (Carissimo et al., 2015; Fragkoudis, Attarzadeh-Yazdi, Nash, Fazakerley, & Kohl, 2009; Lee, Lee, & Lee, 2017; Pasquier, 2005; Schmid-Hempel, 2005; Vilcinskas, 2013; Waldock, Olson, & Christophides, 2012).

One of the most promising elements to face invading pathogens is the ability to unpack DNA to transcribe RNAm and translate a higher protein output to neutralize invading pathogen population (van Zelm, Szczepański, van der Burg, & van Dongen, 2007). In mammals, adaptive responses relies on immune cells entering clonal expansion and antibody affinity selection to cope with the proliferating pathogen population (Bassing, Swat, & Alt, 2002; Sprent, 1994; van Zelm et al., 2007; Weng, Araki, & Subedi, 2012).

In *Drosophila melanogaster* (*Dmel*) the DNA synthesis has been studied in detail during larval and embryonic stages, where mitotic, incomplete mitotic or endoreplication cycles fluctuate in egg chamber in fine regulated mechanisms to developing wings, dorsal polarization and complete egg shell formation (Jia, Tamori, Pyrowolakis, & Deng, 2014; Perdigoto & Bardin, 2013; Shen & Sun, 2017).

Recent research suggests that enteric cells and circulating hemocytes are not only provided by stem cell differentiation during earlier stages, but presence of adult cell clusters progenitor post-larval hematopoiesis relies on Delta-Notch signaling in a similar fashion as in pupal stem cells, and are capable to respond to pathogen challenges (Ghosh, Singh, Mandal, & Mandal, 2015; Guo & Ohlstein, 2015).

In other dipterid, such as *Aedes aegypti*, the midgut adult cells are supposed to not enter mitosis, hence the adaptive-like response observed to recurrent pathogen challenge would imply a genomic change in the challenged cells that would allow the production of effector molecules at a faster pace than the one developed during an only first encounter. We have previously demonstrated that, upon viral challenge and inactive virus oral fed, the mosquito *Aedes aegypti* midgut and carcass cells entered an endoreplication cycle (Serrato-Salas, Hernández-martínez, et al., 2018; Serrato-Salas, Izquierdo-Sánchez, et al., 2018).

This process is controlled by *hnt* gene through Delta-Notch signaling cascade, triggering the genomic DNA synthesis without entering in a mitotic process. The process limits the viral spread to the neighboring cells and is probably related to the progressive diminution of the viral load in the intestinal and somatic cell after the initial infection (Salazar, Richardson, Sánchez-Vargas, Olson, & Beaty, 2007).

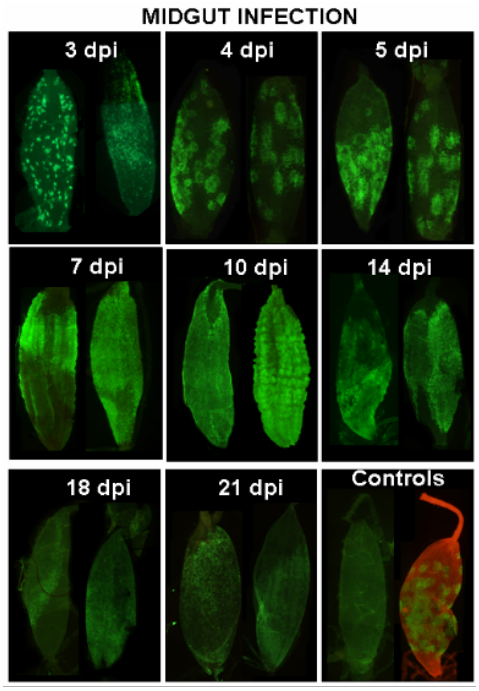

Here we studied the effect of a pathogenic challenge on *Aedes aegypti* culture cells proliferation and immune response.

Materials and methods

Aag-2 cell culture and fungal challenge

Aedes aegypti Aag-2 cells (ATCC CCL-125) were cultured at 28°C in Schneider's *Drosophila* medium for maintenance and microbial challenge. The cell media were supplemented with 10% heat-inactivated fetal bovine serum, 2 mM L-glutamine, and 100 U/mL each of penicillin, streptomycin and neomycin. The monolayer Aag-2 cells were maintained by re-seeding two-three times per week. The cells plates confluence used for assays was minimal 80%. Zymosan-PBS solution was added into the cultured cell medium for 1 h in 24 wells plates.

A proliferation assay was performed for Aag-2 cells treated with different zymosan concentrations at 24 h. The 50% maximum cytotoxic concentration was determined, to test the effects in cells were not caused by direct reduced proliferation.

After incubation, zymosan was removed and replaced with fresh Schneider´s media. The stimulated cells were collected through Trypsin-Versene (Thermo Scientific) partial digestion.

Cells viability assay

Cell viability was determined by trypan blue dye exclusion (0.4% in PBS pH 7.5) in a Neubauer chamber using a bright field microscope. Three-hundred cells were counted for each treatment from five independent experiments done by duplicate.

MTT [4,5 dimethylthiazolil-2]-2,5-diphenyl tetrazolium bromide reduction assays were performed in 96 wells plates. After stimulus, media was removed and replaced with fresh media plus MTT stock solution. After 3 h incubation at 28°C, cells reduced MTT to a formazan insoluble product. Supernatants were transferred to an ELISA plate and solubilized in SDS 10%-HCl 0.01 N solution mix. Optical density was recorded at a 595nm wavelength. At least, five biological assays were performed. Previously, a standard curve calibration was performed to correlate optical density to number of cells.

cDNA synthesis and qPCR strategy

Total RNA from collected Aag-2 cells were performed following protocol instructions from Trizol Reagent (Sigma-Aldrich). Complementary DNA (cDNA) was synthesized for qPCR detection. Quantitative PCR were performed in a ViiA 7 Real-Time PCR System (Applied Biosystems) with the QuantStudio Real Time Software v1.3.

Reactions were realized in a total volume of 10µL containing 5µL of SYBR Green

PCR Master mix, 1.5 ng of cDNA template, 250 nmol of each one of primers, and volume completed with nuclease-free water. Reaction conditions were the following: 50°C for 2 min, 95°C for 10 min followed by 40 cycles of denaturation at 95°C for 15 s, annealing and extension at 60°C for 1 min. The Ct values obtained from the tested gene relative to the reference gene, was used to obtain delta Ct values of zymosan treated and control cell samples. S7 gene (ribosomal unit S70) was selected as the reference gene (Moreno-García, Vargas, Ramírez-Bello, Hernández-Martínez, & Lanz-Mendoza, 2015; Vargas, Moreno-García, Duarte-Elguea, & Lanz-Mendoza, 2016). Relative expression values were obtained using the delta-delta cycle threshold (DDCT) method (Bubner, Gase, & Baldwin, 2004).

We used the PCR primers described in our previous work to quantify the transcription of *hnt* gene upon microbial molecule challenge (Serrato-Salas, Hernández-martínez, et al., 2018; Serrato-Salas, Izquierdo-Sánchez, et al., 2018). Briefly, Ribosomal protein S7 (AAEL009496) 292 bp amplicon; forward 5´ GGG ACA AAT CGG CCA GGC TAT C 3´, reverse 5´ TCG TGG ACG CTT CTG CTT GTT G 3´ primers were used for internal control PCR (Xi, Ramirez, & Dimopoulos, 2008). From CDS and mRNA predicted sequences, following primers were designed: hnt (Fwd): 5´ CGC AAG GAG TTA GAG CGT GA 3´, hnt (Rev): 5´ GTG TCG ATC GCA GTT GGA CT 3´.

Primer	Sequence 5´- 3´	Amplicon size (bp)	Annealing temperature (°C)
Hindsight (Fwd)	5´ GTC CAG TTC TCT ACG GCG C 3´	106	58.1
Hindsight (Rev)	5´ GTG TCG ATC GCA GTT GGA CT 3´		57.4
S7 (Fwd)	5´ GGG ACA AAT CGG CCA GGC TAT C 3´	292	60.2
S7 (Rev)	5´ TCG TGG ACG CTT CTG CTT GTT G 3´		60.1

Genomic DNA extraction

Total genomic DNA (gDNA) was extracted with Phenol-Chloroform-Isoamyl Alcohol mixture according to manufacturer´s instructions. Briefly, the culture cells pools placed in the solvent mixture were homogenized using a small piston until

145 macerated. The phenol interface was washed with citrate buffer. The experimental
146 gDNAs were precipitated with ethanol as per protocol (Hernandez-Martinez et al.,
147 2006; Hernández-Martínez, Barradas-Bautista, & Rodríguez, 2013).
148 gDNA fragmentation
149 The extracted gDNA was subsequently sonicated in a X sonicator, through five 30
150 seconds cycles (on/off) at low power at 4ºC. The gDNA fragmentation was asserted
151 in a 1% agarose gel run in TBE Buffer (Supplementary Material S1).
152 gDNA melting curve
153 The fragmented gDNA melting curves were performed on a Real Time PCR CFX96
154 from Bio-Rad. 5µL of gDNA were mixed with 1µL of Taq buffer and 4µL of SYBR
155 Green PCR Master mix. The mix was subjected to a high-resolution melting analysis
156 from 65ºC to 95ºC at 0.3ºc per second.
157 Agarose pulsed-field electrophoresis
158 Intact cells were embedded in low melting agarose blocks (Schwartz & Cantor 1984).
159 Cells are lysed and proteins are removed by Proteinase K treatment. This procedure
160 yields intact DNA. The agarose block can be loaded directly into the well of a pulsed-
161 field gel. Gels were cast using 1% SeaKem GTG agarose and the electrophoresis
162 performed 24 hours at 120V in 0.5 x TBE buffer. After the completion of the run the
163 agarose gel was stained for 15 min in ethidium bromide (1 mg/ml H_2O). The gel was
164 destained by two washes in 0.5xTBE for 1 hr with gentle agitation and photographed
165 using a shortwave UV-light (254 nm). When the DNA was intended to be used for
166 subsequent restriction and cloning, longwave UV-light (360 nm) was used to avoid
167 nicking of the DNA.
168 **Results**
169 Dose-cytotoxic effect for zymosan-treated cells
170 A proliferation assay for Aag-2 cells treated with different zymosan concentrations for
171 24 h. The half maximum cytotoxic concentration (CC50) value was 34.07-36.91 g/L.
172 (Figure 1A). The final zymosan concentration was 0.5 g/L (70 times lower),
173 confirming that cell effects were not caused by reduced proliferation.
174 Zymosan treatment detains the Aag-2 cells proliferation
175 In order to assess the impact of the signaling mediated by fungal cell wall lysate, we
176 treated Aag-2 cells with zymosan. We counted the cells post challenge and their
177 viability were assessed. The difference in the number of cells counted post treatment
178 points to a stoppage of cells duplication (Figure 1B). These cells were viable, and the

differences of cell number remained equal when counting with MTT assay, hence discarding that the effect would be due to cell death (Figure 1C). Both tests showed that the cell proliferation was detained by the zymosan challenge and that 24 hours after, this difference was bridged. It seems that immune stress does affect cells duplication rate.

Zymosan-mediated cell growth arrest changes the genomic DNA´s cell content

As described in Material and Methods, genomic DNA was obtained through organic solvent extraction (Phenol-Chloroform-Isoamyl alcohol mixture). The total gDNA amount was measured spectrophotometrically (wavelength 260/280 nm) and visualized in agarose gel electrophoresis through EtBr staining. Interestingly, though the number of viable cells was diminished upon zymosan treatment, the total DNA amount per plate increased. The amount of DNA per cell increased, the most prominent difference happening 6 h post challenge, remained at 12 h and recovers control levels at 24 h (Figure 2A). The highest gDNA relative ratio content per cell was observed 6 hours post treatment (Figure 2B).

Zymosan challenge induces *Hnt* gene transcription

Endoreplication phenomena in the *Aedes aegypti* mosquito has been previously observed by our group (Hernandez-Martinez et al., 2006; Hernández-Martínez et al., 2013; Serrato-Salas, Hernández-martínez, et al., 2018; Serrato-Salas, Izquierdo-Sánchez, et al., 2018). We determined that the *hnt* gene transcription correlated with DNA base incorporation in the mosquito cells nuclei (Hernandez-Martinez et al., 2006; Serrato-Salas, Hernández-martínez, et al., 2018). Therefore, we analyzed the *hnt* gene transcription upon microbial challenge. We found that six hours after the zymosan challenge, *hnt* transcript nearly triplicated (Figure 3). Interestingly, the zymosan challenge elicited *hnt* transcription in a timely fashion as to be related with the gDNA/cell increase observed earlier.

Zymosan stimulation altered gDNA sequence proportions

Cell genomic DNA entered an endoreplicating cycle with specific sequences amplified. The melting curve of the extracted gDNA showed diverging pattern in control and zymosan challenged Aag-2 culture cells. If the phenomenon would have implied a gDNA duplication, the proportion of each genomic sequences would have been equal hence their melting curves also. As can be observed in Figure 4, The melting curve of the sonicated gDNA of control and induced cells are different. The fact that some lower temperature peaks are bigger in zymosan treated cells point to

an increase in the number of specific sequences against the rest of the genome, suggesting that only specific part of the genome are amplified. The melt temperature of the control samples was 75.06 +- 2.1 ºc while the zymosan treated gDNA had a melt temperature of 66.52+-3.2 ºc. This could be due to the relative amount of repeated sequences of the endoreplicated sequences that would separate jointly at a lower temperature than the non endoreplicated gDNA part.

Zymosan stimulated *Aag2* cells gDNA present lower molecular weight DNA

The later evidences pointed to the amplification of specific gDNA regions by the *Aag2* cells submited to the zymosan stress. The partial gDNA amplification implied the presence of large extrachromosomal DNA sequences in the treated cells nucleus. Therefore, we separate the chromosomal DNA by pulse field chromatography, expecting to see large DNA fragment in the gDNA of the treated cells. As can be seen in figure 5, we did observe such fragment in the treated cell gDNA between 25 and 35 kBases.

Conclusion

Aag-2 cells is a model for *Aedes aegpyti* competent immune response. Immune challenge induces cell division arrest in these cells. The relative genomic DNA content transiently increases at the same time that *hnt* gene transcription increases. The DNA content increase is related to specific genomic sequence amplification, the same are transient and resolved 24 hours post immune stress.

Figure 1

A

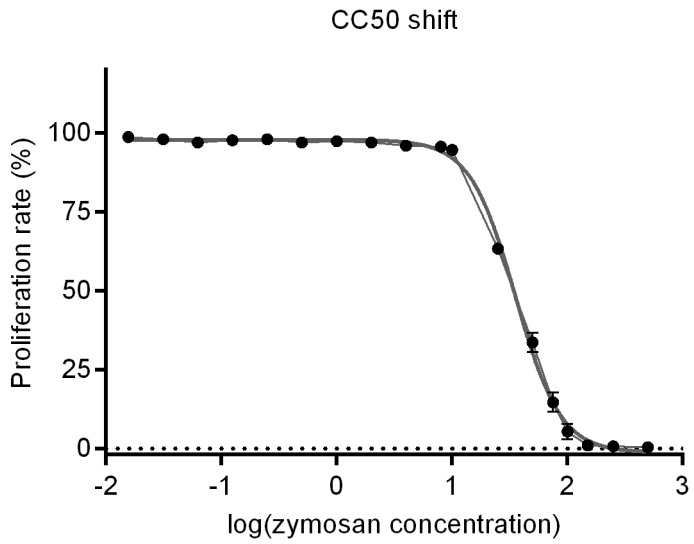

B

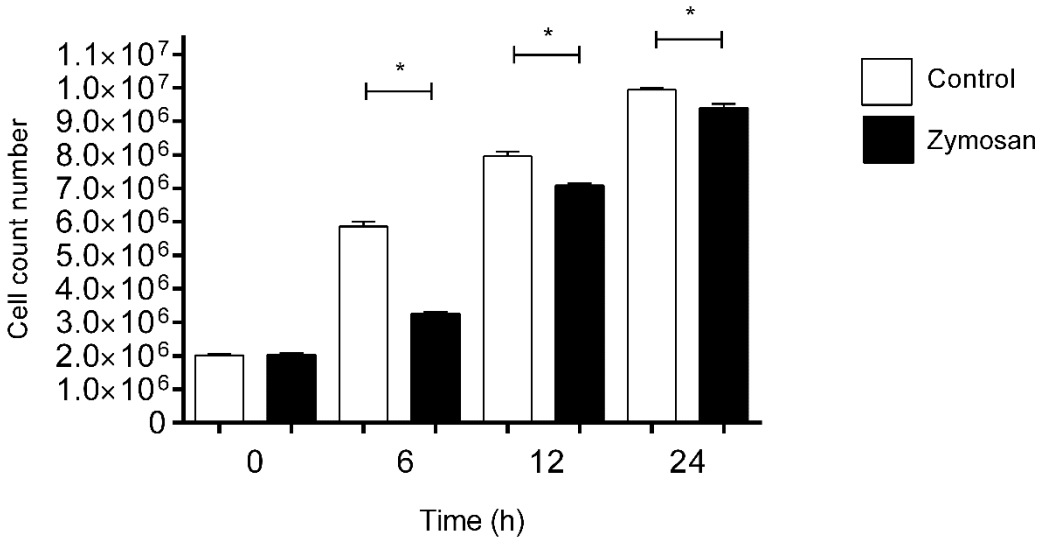

C

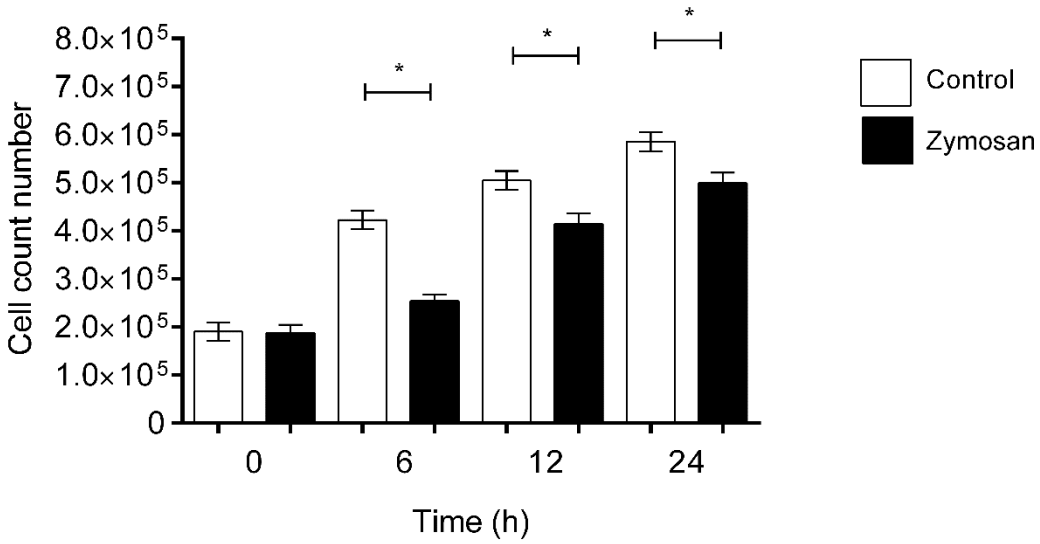

Fig. 1: A) Cytotoxic concentration assay. LogCC50 1.532-1.567 (CC50 34.07-36.91 g/L). R^2 = 0.9977. B) Aag-2 cells number per culture plate over 24 hours post zymosan challenge. Student´s T-test with Welch´s correction 0 h p=0.7148. 6 h p<0.0001. 12 h p<0.0001. 24 h p<0.0001. C) MTT exclusion dye viable cell number per culture plate over 24 hours post zymosan challenge. Student T-test welch correction values are for 0 h time point p=0.6694; 6 h p<0.0001; 12 h p<0.0001, 24 h p<0.0001.

Fig. 2

A

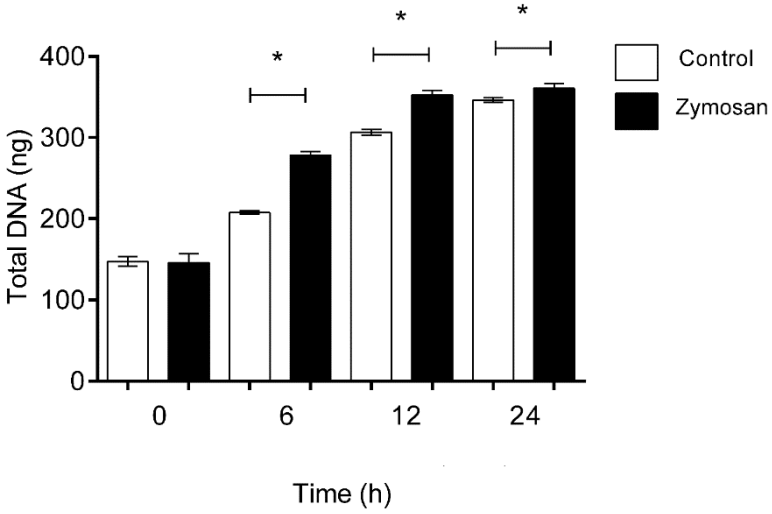

B

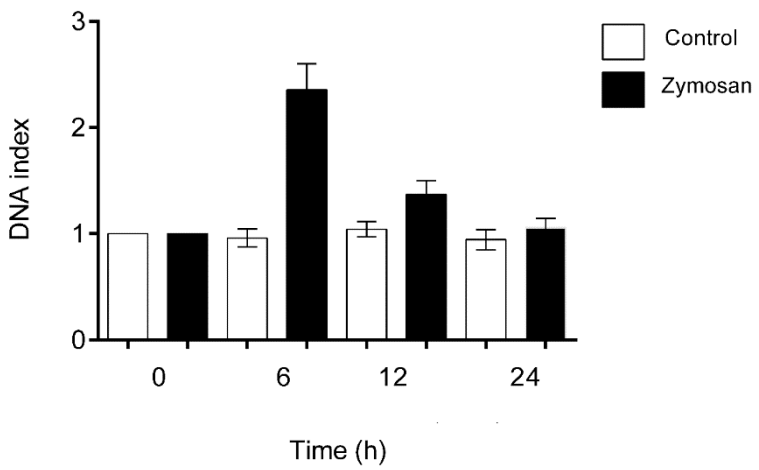

Figure 2: A) Total gDNA amount extracted from the cell cultures at 0, 6, 12 and 24 hours post zymosan challenge. 0 h p=0.6676. 6 h p<0.0001. 12 h p<0.0001. 24 h p<0.0001.

B) Normalized relative gDNA content per cell at 0, 6, 12 and 24 hours post zymosan challenge.

Fig. 3

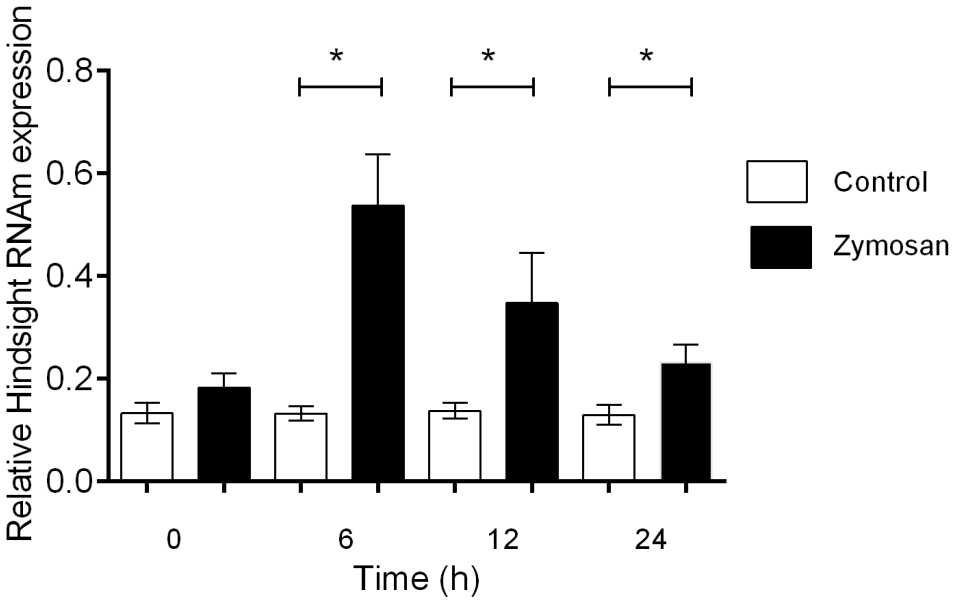

Figure 3: Relative *Hindsight* gene transcription post challenge. The transcripts amount values were normalized against ribosomal S7 gen. 0 h p=0.0001. 6 h p<0.0001. 12 h p<0.0001. 24 h p<0.0001.

Figure 4

A

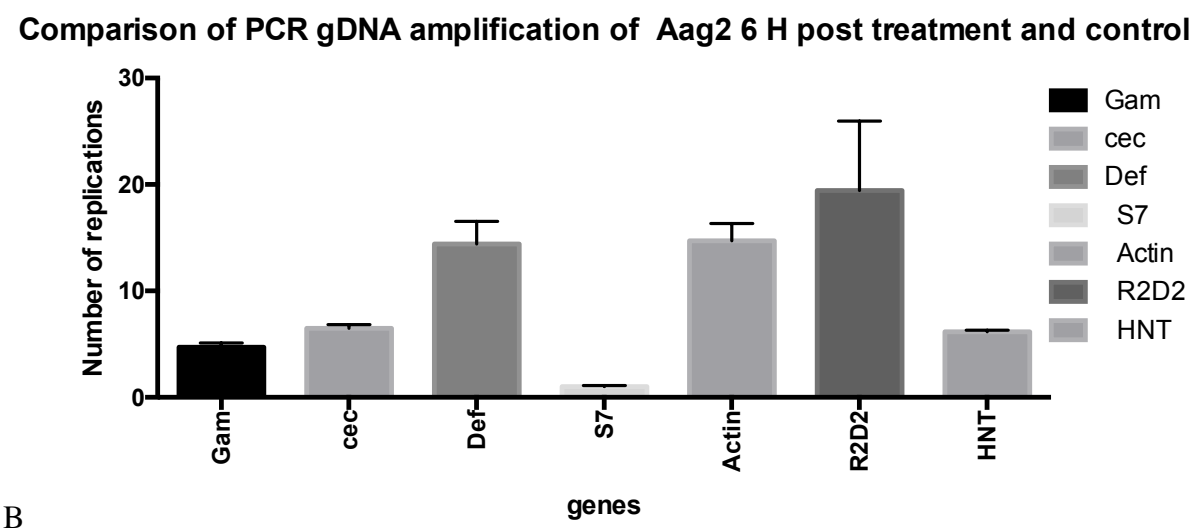

B

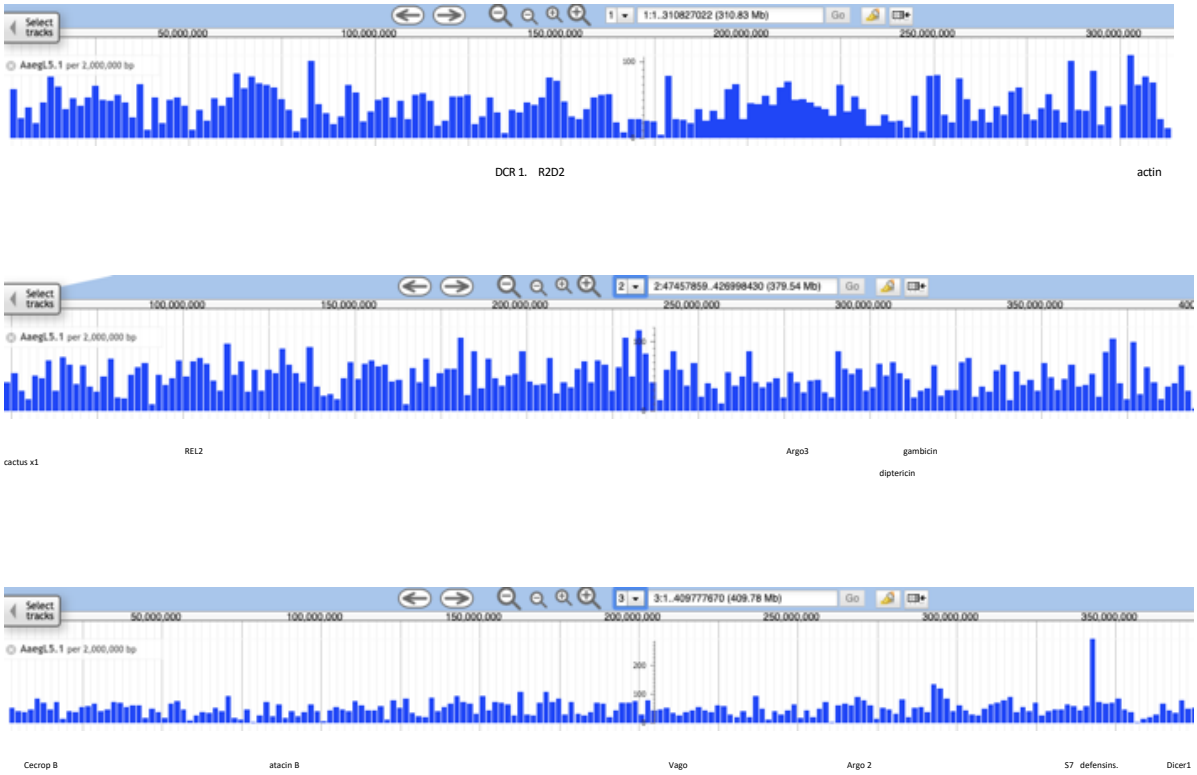

Fig.4 A Genomic PCR of distinct *Aedes* genes. The amplification of the same amount of gDNA was relativized to the gene that needed the most cycle to appear: S7. 4B Genomic distribution of the genes sequence chosen for gDNA qPCR.

Fig. 5

A)

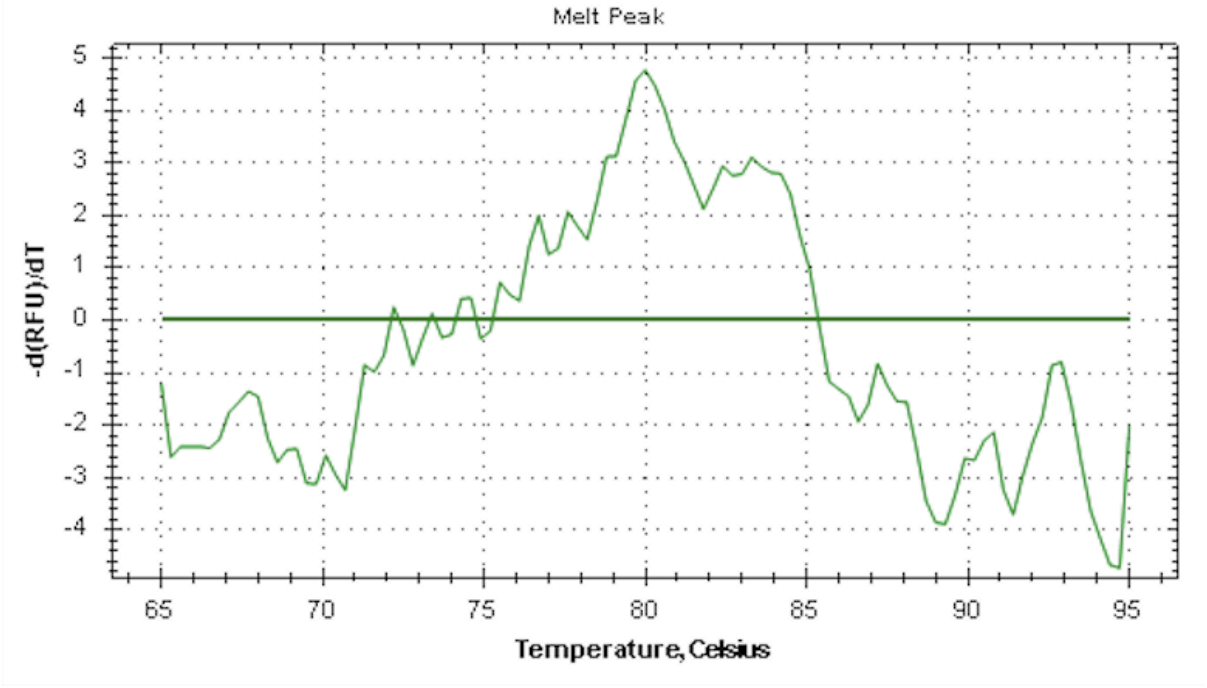

B)

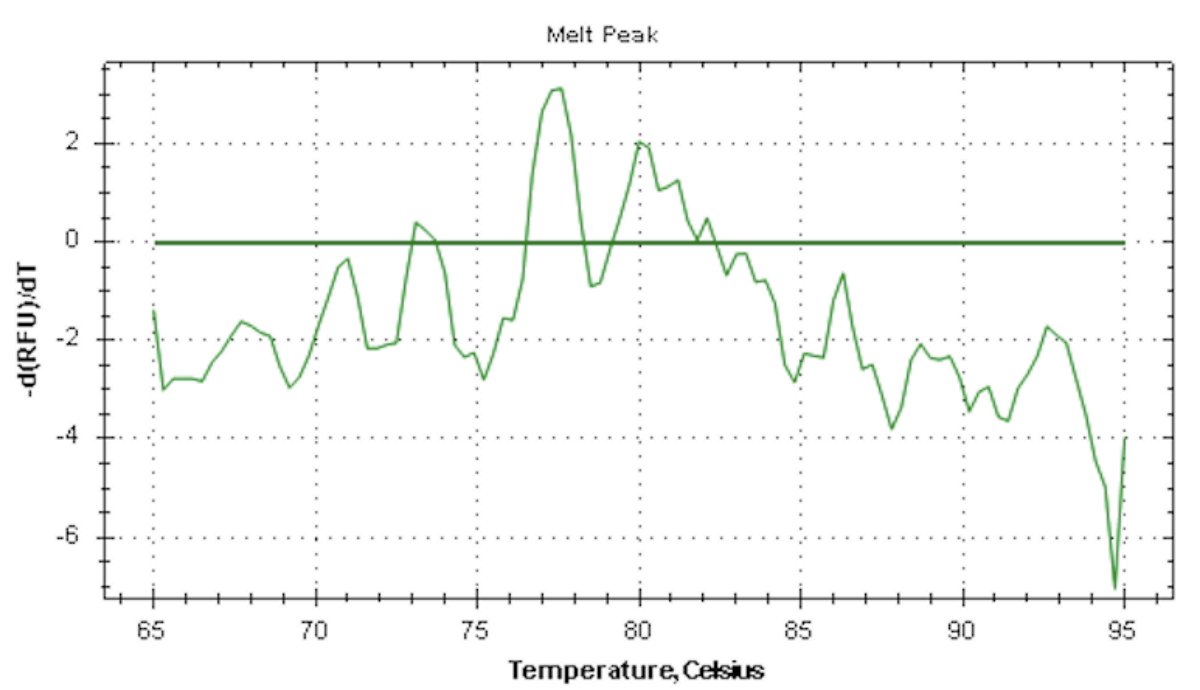

Figure 4. Melt peaks of sonicated cultured cells gDNA A) in control conditions B) six hours post Zymosan exposure.

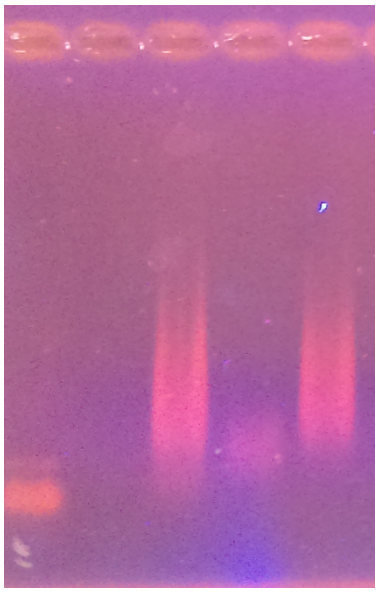

Figure S1: Aag-2 cells gDNA fragmentation.

Fig. 5

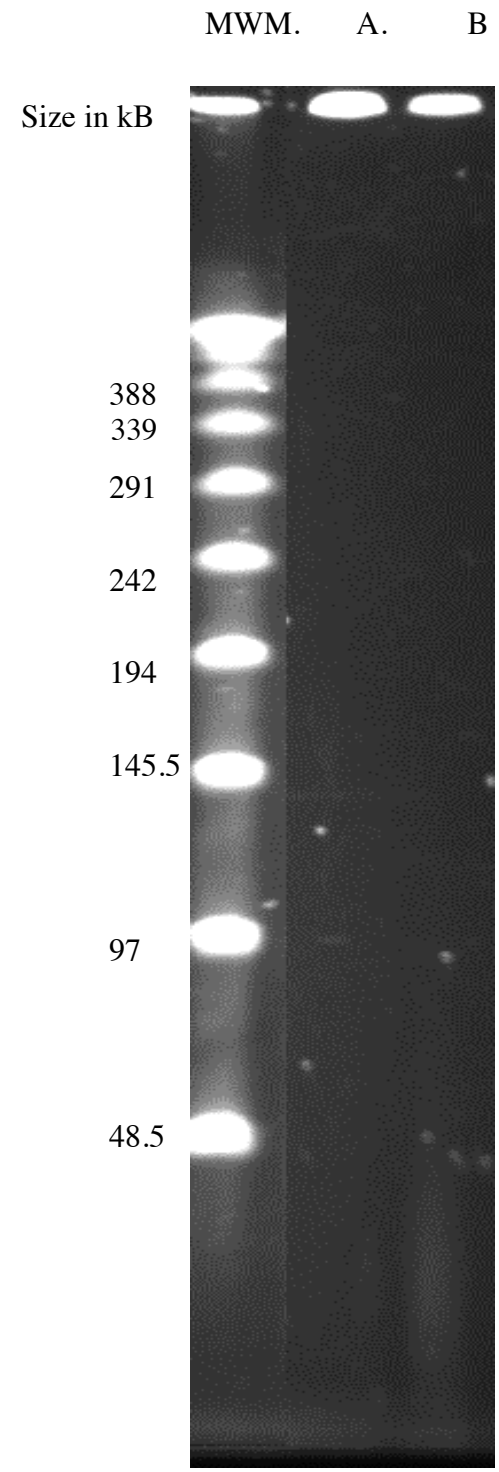

Figure 5: Pulsed field gel of the *Aag2* cells gDNA Control (A) and 6 hours post Zymozan challenge (B).

397 Fig.6

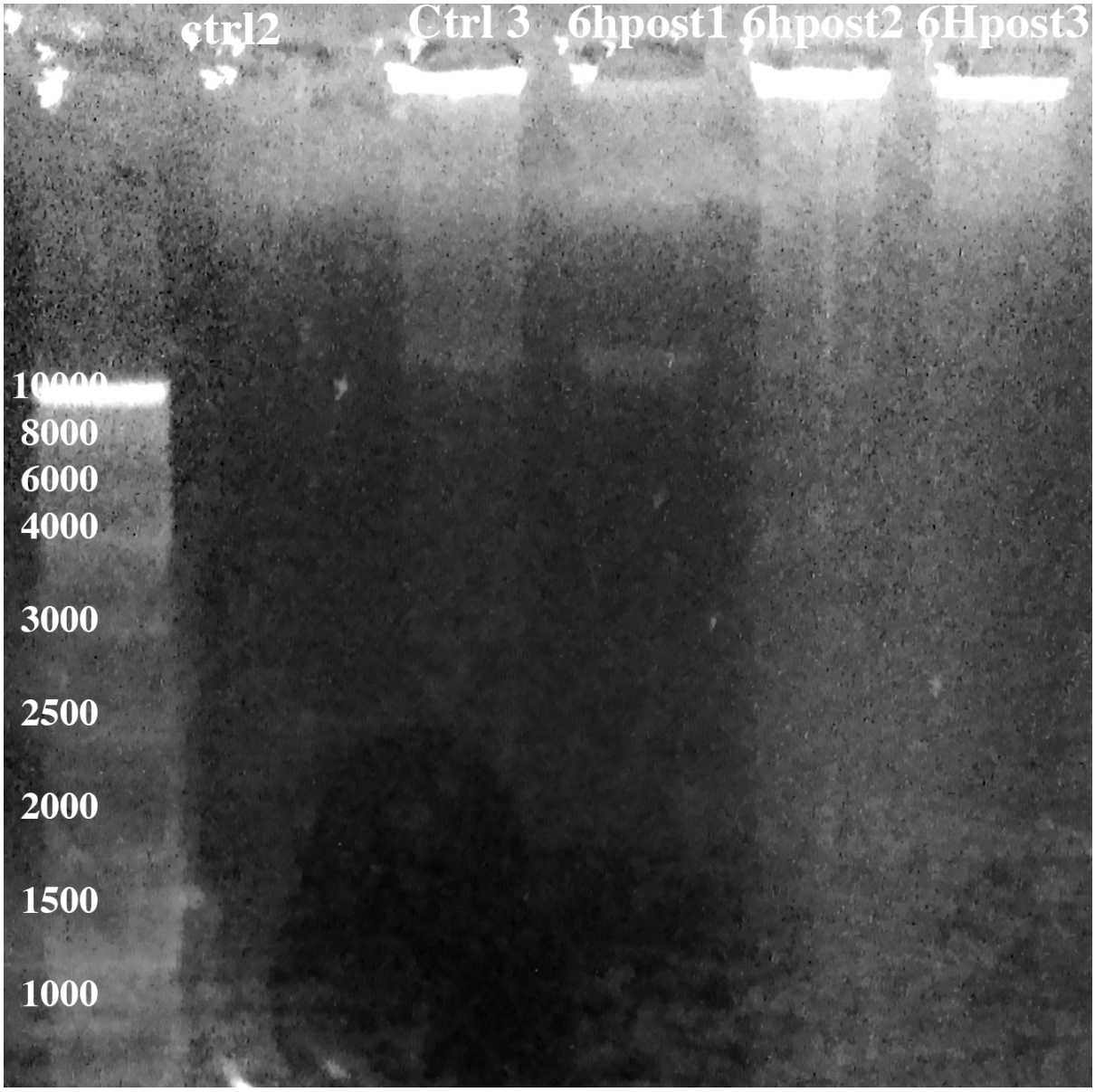

398

399 Fig. 6: gDNA of control and zymosan treated cells.

400

Fig. S.2

A)

B)

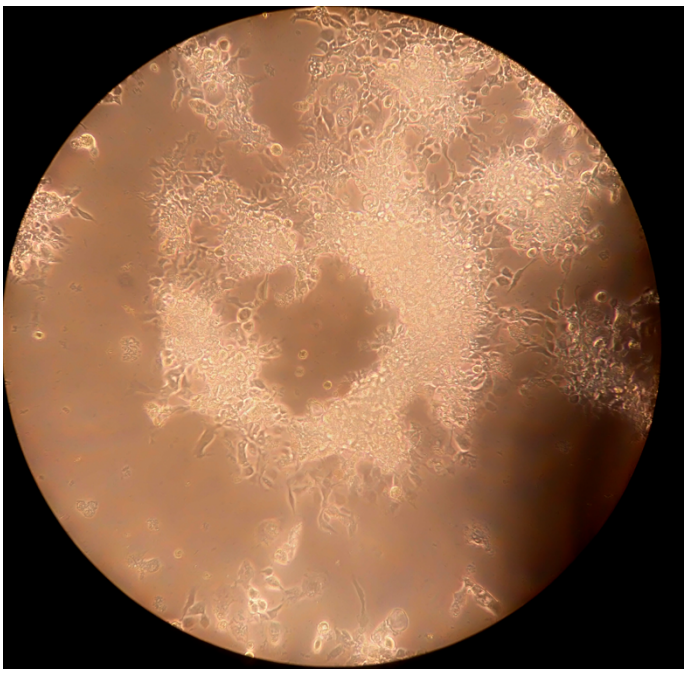

S2: Aag2 culture cells 20X pictures. A) control, B) six hours post zymosan treatment.

References

Barnard, A. C., Nijhof, A. M., Fick, W., Stutzer, C., & Maritz-Olivier, C. (2012). RNAi in arthropods: Insight into the machinery and applications for understanding the pathogen-vector interface. *Genes*, *3*(4), 702–741. https://doi.org/10.3390/genes3040702

Bassing, C. H., Swat, W., & Alt, F. W. (2002). The mechanism and regulation of chromosomal V(D)J recombination. *Cell*, *109 Suppl*(D), S45-55.

Bubner, B., Gase, K., & Baldwin, I. T. (2004). Two-fold differences are the detection limit for determining transgene copy numbers in plants by real-time PCR. *BMC Biotechnology*, *4*, 14. https://doi.org/10.1186/1472-6750-4-14 1472-6750-4-14 [pii]

Burnet, F. M. (1976). A Modification of Jerne's Theory of Antibody Production using the Concept of Clonal Selection. *CA: A Cancer Journal for Clinicians*, *26*(2), 119–121. https://doi.org/10.3322/canjclin.26.2.119

Carissimo, G., Pondeville, E., McFarlane, M., Dietrich, I., Mitri, C., Bischoff, E., … Vernick, K. D. (2015). Antiviral immunity of *Anopheles gambiae* is highly compartmentalized, with distinct roles for RNA interference and gut microbiota. *Proceedings of the National Academy of Sciences*, *112*(2), E176–E185. https://doi.org/10.1073/pnas.1412984112

Costa, A., Jan, E., Sarnow, P., & Schneider, D. (2009). The Imd pathway is involved in antiviral immune responses in Drosophila. *PLoS ONE*, *4*(10). https://doi.org/10.1371/journal.pone.0007436

De Gregorio, E., Spellman, P. T., Tzou, P., Rubin, G. M., & Lemaitre, B. (2002). The Toll and Imd pathways are the major regulators of the immune response in Drosophila. *EMBO Journal*, *21*(11), 2568–2579. https://doi.org/10.1093/emboj/21.11.2568

Dong, Y., Aguilar, R., Xi, Z., Warr, E., Mongin, E., & Dimopoulos, G. (2006). Anopheles gambiae immune responses to human and rodent Plasmodium parasite species. *PLoS Pathogens*, *2*(6), 0513–0525. https://doi.org/10.1371/journal.ppat.0020052

Fragkoudis, R., Attarzadeh-Yazdi, G., Nash, A. A., Fazakerley, J. K., & Kohl, A. (2009). Advances in dissecting mosquito innate immune responses to arbovirus infection. *Journal of General Virology*, *90*(9), 2061–2072. https://doi.org/10.1099/vir.0.013201-0

Ghosh, S., Singh, A., Mandal, S., & Mandal, L. (2015). Active Hematopoietic Hubs in Drosophila Adults Generate Hemocytes and Contribute to Immune Response. *Developmental Cell*, *33*(4), 478–488. https://doi.org/10.1016/j.devcel.2015.03.014

Guo, Z., & Ohlstein, B. (2015). Bidirectional Notch signaling regulates Drosophila intestinal stem cell multipotency. *Science*, *350*(6263), 927. https://doi.org/10.1126/science.aab0988

Hernández-Martínez, S., Barradas-Bautista, D., & Rodríguez, M. H. (2013). Diferential DNA Synthesis In Anopheles Albimanus Tissues Induced By Immune Challenge With Different Microorganisms. *Archives of Insect Biochemistry and Physiology*, *84*(1), 1–14. https://doi.org/10.1002/arch.21108

Hernandez-Martinez, S., Román-Martínez, U., Martínez-Barnetche, J., Garrido, E., Rodríguez, M. H., & Lanz-Mendoza, H. (2006). Induction of DNA synthesis in Anopheles albimanus tissue cultures in response to a Saccharomyces cerevisiae challenge. *Archives of Insect Biochemistry and Physiology*, *63*(4), 147–158. https://doi.org/10.1002/arch.20150

Hillyer, J. F. (2010). MOSQUITO IMMUNITY (pp. 218–238).

Jia, D., Tamori, Y., Pyrowolakis, G., & Deng, W. M. (2014). Regulation of broad by the Notch pathway affects timing of follicle cell development. *Developmental Biology*, *392*(1), 52–61. https://doi.org/10.1016/j.ydbio.2014.04.024

Kleino, A. (2010). *The Imd Pathway-mediated Immune Response in Drosophila*.

Lee, J. H., Lee, K. A., & Lee, W. J. (2017). *Microbiota, Gut Physiology, and Insect Immunity*. *Advances in Insect Physiology* (1st ed., Vol. 52). Elsevier Ltd. https://doi.org/10.1016/bs.aiip.2016.11.001

Moreno-García, M., Vargas, V., Ramírez-Bello, I., Hernández-Martínez, G., & Lanz-Mendoza, H. (2015). Bacterial Exposure at the Larval Stage Induced Sexual Immune Dimorphism and Priming in Adult Aedes aegypti Mosquitoes. *PloS One*, *10*(7), e0133240. https://doi.org/10.1371/journal.pone.0133240

Pasquier, L. Du. (2005). Insects Diversify One Molecule to Serve Two Systems, (September), 1826–1827.

Perdigoto, C. N., & Bardin, A. J. (2013). Sending the right signal: Notch and stem cells. *Biochimica et Biophysica Acta - General Subjects*, *1830*(2), 2307–2322. https://doi.org/10.1016/j.bbagen.2012.08.009

Salazar, M. I., Richardson, J. H., Sánchez-Vargas, I., Olson, K. E., & Beaty, B. J. (2007). Dengue virus type 2: replication and tropisms in orally infected Aedes aegypti mosquitoes. *BMC Microbiology*, *7*, 9. https://doi.org/10.1186/1471-2180-7-9

Schmid-Hempel, P. (2005). Evolutionary Ecology of Insect Immune Defenses. *Annual Review of Entomology*, *50*(1), 529–551. https://doi.org/10.1146/annurev.ento.50.071803.130420

Serrato-Salas, J., Hernández-martínez, S., Martínez-barnetche, J., Condé, R., Alvarado-delgado, A., Zumaya-estrada, F., & Lanz-mendoza, H. (2018). De Novo DNA Synthesis in Aedes aegypti Midgut Cells as a Complementary Strategy to Limit Dengue Viral Replication, *9*(April), 1–12. https://doi.org/10.3389/fmicb.2018.00801

Serrato-Salas, J., Izquierdo-Sánchez, J., Argüello, M., Conde, R., Alvarado-Delgado, A., & Lanz-Mendoza, H. (2018). Aedes aegypti antiviral adaptive response against DENV-2. *Developmental & Comparative Immunology*, *84*, 28–36. https://doi.org/10.1016/j.dci.2018.01.022

Shen, W., & Sun, J. (2017). Dynamic Notch Signaling Specifies Each Cell Fate in Drosophila Spermathecal Lineage. *G3 (Bethesda, Md.)*, *7*(5), 1417–1427. https://doi.org/10.1534/g3.117.040212

Sprent, J. (1994). T and B memory cells. *Cell*, *76*(2), 315–22. https://doi.org/0092-8674(94)90338-7 [pii]

van Zelm, M. C., Szczepański, T., van der Burg, M., & van Dongen, J. J. M. (2007). Replication history of B lymphocytes reveals homeostatic proliferation and extensive antigen-induced B cell expansion. *The Journal of Experimental Medicine*, *204*(3), 645–655. https://doi.org/10.1084/jem.20060964

Vargas, V., Moreno-García, M., Duarte-Elguea, E., & Lanz-Mendoza, H. (2016). Limited Specificity in the Injury and Infection Priming against Bacteria in Aedes aegypti Mosquitoes. *Frontiers in Microbiology*, *7*, 975. https://doi.org/10.3389/fmicb.2016.00975

Vilcinskas, A. (2013). Evolutionary plasticity of insect immunity. *Journal of Insect Physiology*, *59*(2), 123–9. https://doi.org/10.1016/j.jinsphys.2012.08.018

517 Waldock, J., Olson, K. E., & Christophides, G. K. (2012). Anopheles gambiae antiviral
518 immune response to systemic O'nyong-nyong infection. *PLoS Neglected Tropical*
519 *Diseases*, *6*(3). https://doi.org/10.1371/journal.pntd.0001565

520 Weavers, H., Evans, I. R., Martin, P., & Wood, W. (2016). Corpse Engulfment Generates a
521 Molecular Memory that Primes the Macrophage Inflammatory Response. *Cell*, *165*(7),
522 1658–1671. https://doi.org/10.1016/j.cell.2016.04.049

523 Weng, N., Araki, Y., & Subedi, K. (2012). The molecular basis of the memory T cell
524 response: differential gene expression and its epigenetic regulation. *Nature Reviews*
525 *Immunology*, *12*(4), 306–315. https://doi.org/10.1038/nri3173

526 Xi, Z., Ramirez, J. L., & Dimopoulos, G. (2008). The Aedes aegypti toll pathway controls
527 dengue virus infection. *PLoS Pathogens*. https://doi.org/10.1371/journal.ppat.1000098

528